

Prenatal phthalate exposures and adiposity outcomes trajectories: a multivariate Bayesian factor regression approach

Phuc Nguyen, Stephanie M. Engel, Amy H. Herring

June 12, 2025

Abstract

We aim to assess the longitudinal effects of prenatal exposure to phthalates on the risk of childhood obesity in children aged 4 to 7, with potential time-varying and sex-specific effects. Multiple body-composition-related outcomes, such as BMI z-score, fat mass percentage, and waist circumference, are available in the data. Existing chemical mixture analyses often look at these outcomes individually due to the limited availability of multivariate models for mixture exposures. We propose a multivariate Bayesian factor regression that handles multicollinearity in chemical exposures and borrows information across highly correlated outcomes to improve estimation efficiency. We demonstrate the proposed method's utility through simulation studies and an analysis of data from the Mount Sinai Children's Environmental Health Study. We find the associations between prenatal phthalate exposures and adiposity outcomes in male children to be negative at early ages but to become positive as the children get older.

Key Words: Bayesian factor model, multivariate regression, longitudinal data, chemical mixtures.

1 Introduction

The increasing prevalence of childhood obesity is a relevant public health concern. The 2017-2018 National Health and Nutrition Examination Surveys (NHANES) estimated that 19.3% of children aged 2-19 years have obesity and another 16.1% are overweight (Fryar et al., 2020). The prevalence of obesity among children and adolescents has increased by over threefold in the last 30 years (Committee on Accelerating Progress in Obesity Prevention and others, 2012). Obese children are at greater risk for several health conditions, including obesity in adulthood, type 2 diabetes, heart disease, arthritis, various cancers, and a shorter lifespan. Studies suggest that approximately 70% of obese children face a significant risk of heart diseases in adulthood (Gollust et al., 2013). Some estimates suggest that one-third of children born today (and half of Latino and black

children) are expected to develop type 2 diabetes at some point in their lives (Narayan et al., 2003). Childhood obesity also carries negative implications for mental health, as it is linked to an increased risk of being bullied (Gollust et al., 2013).

Environmental chemical exposures have been found to increase the risk of obesity in children by interfering with the body’s hormones, also known as the endocrine system. Currently, over 800 chemicals are known to be endocrine-disrupting. At least 33 epidemiological studies on humans have established a connection between developmental exposure to environmental chemicals and weight gain among children during their later years (National Academies of Sciences, Engineering, and Medicine and others, 2016; Vrijheid et al., 2020). Exposures to endocrine-disrupting chemicals are also common in newborn babies and pregnant women (National Academies of Sciences, Engineering, and Medicine and others, 2016). The human body is most vulnerable to the long-lasting effects of environmental chemical exposure during development in utero and early childhood (National Academies of Sciences, Engineering, and Medicine and others, 2016). For example, exposures to obesogens, such as cigarette smoke, and diethylstilbestrol, during gestational or postnatal periods have been shown to associate with childhood obesity, even after the chemicals had been eliminated (National Academies of Sciences, Engineering, and Medicine and others, 2016).

Phthalates are a group of chemicals commonly used in consumer products, such as toys, food packaging, or cosmetics, that are known to have endocrine-disrupting properties. Exposure to phthalates is often approximated by measurement of concentrations of phthalate metabolites in urine (Kim and Park, 2014). In vivo and in vitro studies suggest that exposure to phthalates, notably di-2-ethylhexyl phthalate (DEHP) metabolites, may promote obesity, and the effect may depend on gender and exposure period, with fetal development a potential critical window (Kim and Park, 2014; National Academies of Sciences, Engineering, and Medicine and others, 2016). There is also a large body of literature on observational studies of phthalate exposures in humans (Golestanzadeh et al., 2019). Cross-sectional studies using NHANES have found associations, including age, gender, and racial differences in the associations, between phthalate mixtures and adiposity outcomes (Trasande et al., 2013; Buser et al., 2014; Wu et al., 2020; Berger et al., 2021; Seo et al., 2022). Because pregnancy is a vulnerable period of exposure, many prospective studies have examined how prenatal exposures to phthalates affect newborns and young children. They also observed adverse effects on adiposity outcomes and sex-specific effects, though phthalate components identified as critical differed between studies (Buckley et al., 2016a; Vafeiadi et al., 2018; Berger et al., 2021). However, how the health effects of prenatal exposures to phthalates change as a child grows up, for instance, whether the effects dampen or intensify over time, is less well-studied.

While existing approaches shed light on various aspects of the mixtures’ health effects over time, they also have unique limitations. Studies that fitted single-metabolite models with time-varying effects (Harley et al., 2017) failed to account for the fact that subjects were exposed to all phthalates metabolites simultaneously. Many studies fitted multi-metabolites linear mixed-effects

models with interactions between chemicals and age, or fractional polynomials of age (Yang et al., 2018; Ye’elah et al., 2021). Linear mixed models are not well-suited to model the health effects of highly correlated phthalate mixtures. They can produce unstable estimates under minor changes to model specification in the presence of multicollinearity (Bobb et al., 2015). A common workaround is to take the molar sum of correlated groups such as DEHP (Buckley et al., 2016b; Harley et al., 2017; Ye’elah et al., 2021), low molecular weight phthalates, or high molecular weight phthalates (Trasande et al., 2013; Buser et al., 2014; Ye’elah et al., 2021), or preprocess the exposures with principal component analysis (PCA) (Maresca et al., 2016). However, analyzing the molar sum implies that we believe all components within the sum are equally important to predicting the outcome. Additionally, PCA finds directions that explain the most variability in the mixtures, not necessarily those most highly associated with the outcome. It is desirable to have models that infer groups of chemicals most correlated to the outcome.

Heggeseth et al. (2019) used more advanced methods, including generalized additive models (GAM), growth mixture models (GMM), and functional PCA (FPCA) with random forest (RF), to find non-linear effects of prenatal exposures on BMI trajectories up to puberty. These methods also have unique limitations for estimating time-varying effects. GAM is flexible and can model nonlinear effects and interactions at each follow-up time point, however, it does not directly model effects over time (Heggeseth et al., 2019). GMM infers latent group membership for each subject and estimates group-specific, potentially nonlinear, outcome trajectories and their relationships to exposures (Jung and Wickrama, 2008). As a result, it would be overly complex if the focus is on estimating a single average relationship over time between the exposures and outcomes in the study population. Due to GMM’s complexity, Heggeseth et al. (2019) fitted one separate model for each exposure, limiting the approach from accounting for joint effects of or interactions between exposures. FPCA provides functions that maximize variation in the outcomes trajectories, though these may not maximize associations with the exposures (Heggeseth et al., 2019). FPCA scores, which are numerical summaries of the outcome trajectories, can be regressed by exposure mixtures and covariates using RF. Though RF is flexible, can model nonlinear, synergistic effects, and selects for important predictors, it lacks interpretability. RF produces relative variable importance and requires multi-perspective visualizations or post hoc methods for interpretations of effects (Haddouchi and Berrado, 2019). While these advanced methods can model outcome trajectories, it is not intuitive to interpret how the effects of chemicals change over time from their results.

Bayesian varying coefficient kernel machine regression (BVCKMR), another advanced mixture method, can model non-linear, non-additive effects on the outcome and outcome’s trajectories (Liu et al., 2018). BVCKMR works with univariate outcomes. It has not been used to study phthalates mixtures’ effects on obesity, though it was applied in other exposure mixtures studies (Howe et al., 2021; Colicino et al., 2022). Prior research has shown that incorporating grouping structures (e.g. groups of highly correlated chemicals such as DEHP)

within the kernel machine framework improved the power to detect associations (Bobb et al., 2015), though this feature is not available in BVCKMR. Additionally, fixing the levels of the exposures, BVCKMR assumes the change in an effect over time is constant.

Another limitation in the current literature is the lack of analysis considering multiple adiposity outcomes simultaneously. Several outcomes, such as BMI, waist circumference, and fat mass percentage, are often available in a data set. Previous studies largely examine their associations with phthalate exposures individually (Maresca et al., 2016; Buckley et al., 2016a; Harley et al., 2017; Vafeiadi et al., 2018; Bowman et al., 2019; Berger et al., 2021; Ye’elah et al., 2021). At the same time, they often hypothesized mixtures to have similar effects on all outcomes (Maresca et al., 2016) or looked for consistent estimates across outcomes when interpreting the results (Harley et al., 2017; Berger et al., 2021; Ye’elah et al., 2021). As these measurements are highly correlated and are driven by similar mechanisms through which phthalates affect obesity, we can expect to improve estimation efficiency by modeling them jointly. Many benefits of the joint modeling approach have been studied in the multi-task learning problem in the machine learning literature (Zhang and Yang, 2018). This necessitates multivariate models that can handle multicollinearity in the exposures.

To address these limitations, we study time-varying effects of prenatal exposures to phthalates on several childhood adiposity outcomes jointly using data from the Mount Sinai Children’s Environmental Health Study (MSCEHS) (Engel et al., 2007; Buckley et al., 2016a). The study measured urinary phthalates metabolites during the third trimester of pregnancy and followed up on the children’s health indices, including adiposity outcomes, at three time points. We would like to identify groups of phthalate mixtures critical to all adiposity outcomes and estimate their time-varying effects and any sex-specific effects.

To this end, we introduce a Bayesian multivariate factor regression model for time-varying effects. The model assumes structured variations in correlated chemical mixtures can be attributed to a small number of latent factors that also explains part of the variations in the correlated outcomes. We expect our method to be a good alternative when the effects of the latent factors on the outcomes are correlated across outcomes, for example because they affect the outcomes through the same causal pathway. However, it may not be ideal when outcomes are unrelated, or when different chemicals affect different outcomes. This provides supervised learning of common factors that predicts the outcomes, as well as propagate the uncertainty in the factors to the regression. On the other hand, PCA components or molar sums that are entirely informed by the structures of the exposures and the analyst’s intuition. Finally, if there is interest in identifying potentially non-linear changes in the effects over time, our model directly estimates effects as smooth functions of time, making it more interpretable than alternatives. Section 2 describes in detail data from the MSCEHS. Section 3 describes our proposed model and its prior specifications. Section 4 and Section 5 shows utility of the proposed model using simulation studies and an analysis of the MSCEHS data.

2 Data

Study population

Between 1998 and 2002, the MSCEHS recruited 479 first-time mothers with singleton pregnancies from the Mount Sinai Diagnostic and Treatment Center and two adjacent private practices in New York City. After excluding 75 women (see details in [Engel et al. \(2007\)](#)), the final cohort consisted of 404 babies with recorded birth data. The children were invited back for three follow-up visits at ages 4-5.5, 6, and 7-9. Of the 404 babies, 382 had their mothers' prenatal phthalate metabolite concentrations measured in urine. Two additional observations were excluded because they had very dilute urine (< 10 mg/dL creatinine) that may produce inaccurate biomarker measurements ([Buckley et al., 2016a](#)). Of the 382 babies, only 180 came back for at least one follow-up visit. This results in 362 total visits for fat mass percentage, 363 total visits for body mass index (BMI), 364 total visits for waist-to-hip ratio, and 364 total visits for waist circumference. Figure 1 shows the pattern of loss to follow-up of these 382 babies. These observations are included in our analysis. The study was approved by the Mount Sinai School of Medicine Institutional Review Board. The women gave written consent, and children aged seven or older gave their assent to participate ([Buckley et al., 2016a](#)).

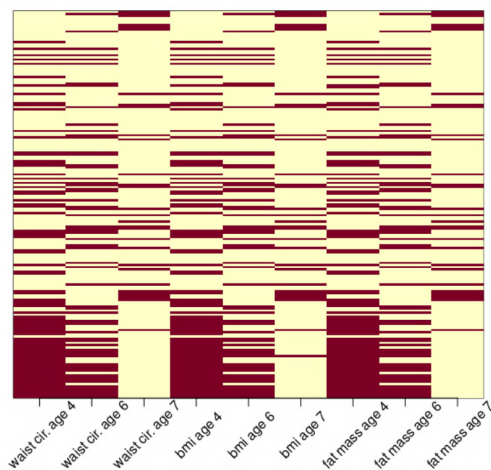


Figure 1: Loss to follow-ups patterns for WC, BMI, and FMP in the study population. Maroon indicates observed time point.

Phthalate exposures

Mothers who were pregnant between 25 and 40 weeks (with a mean of 31.5 weeks) provided a urine sample that was analyzed for various phthalate metabolites by the CDC laboratory, including MEP, MnBP, MiBP, MCP, MBzP,

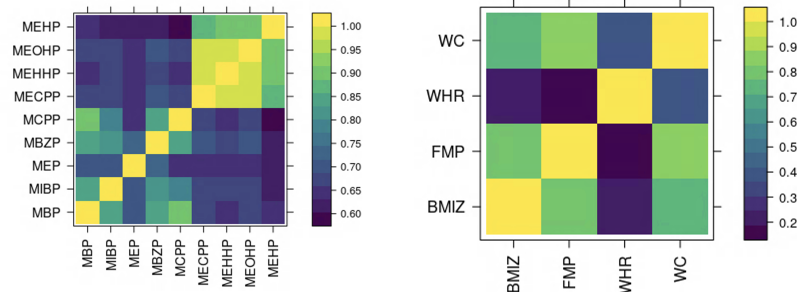


Figure 2: Left: Sample correlation of phthalate metabolites concentrations. Right: Sample correlation of adiposity outcomes.

MEHP, MEHHP, MEOHP, and MECPP. The DEHP group consists of MEHP, MEHHP, MEOHP, and MECPP. To account for inaccuracies in analytical standards, correction factors of 0.72 and 0.66 were applied to MBzP and MEP concentrations and limits of detection (LOD) respectively (CDC, 2012). Urinary concentration was measured using creatinine. To adjust for the dilution of urine samples, we standardize the metabolites' concentrations by a Cratio, as well as include creatinine concentration as a covariate in your analysis as suggested by O'Brien et al. (2017). The Cratio is calculated as the ratio between predicted (by observed covariates) and observed creatinine (O'Brien et al., 2017). As seen in Figure 2 (Left), phthalate metabolites are highly correlated with each other, especially those within the DEHP group and those within the non-DEHP group. There are 4 MiBP, 1 MEP, 1 MBzP, 4 MCPP, 1 MECPP, 1 MEHHP, 1 MEOHP, and 15 MEHP measurements under their respective LOD of detections in total. We impute these within the MCMC sampler as discussed later.

Adiposity outcomes

The MSCEHS assessed the weight and body composition of the infants through bioelectrical impedance analysis using a pediatric Tanita scale at three follow-up visits scheduled at approximately 4 years, 6 years, and 7 years, though the age the children at actual visits ranges from 4 to 10 years (or 48 to 122 months). We consider the following four outcomes in our multivariate analysis: fat mass percentage (FMP), BMI z-score (BMIZ), waist-to-hip ratio (WHR), and waist circumference (WC). FMP is based on fat mass estimates reported by the Tanita scale (model TBF-300; Tanita Corporation of America) and calculated as $(\text{fat mass}/\text{weight}) \times 100$. BMI is calculated as $\text{weight (in kilograms)}/\text{height (in meters)}^2$. It is then standardized by age and sex using a CDC SAS macro (CDC, 2004) to produce BMIZ. There are 362 total visits for FMP, 363 for BMIZ, 364 for WHR, and 364 for WC from 180 subjects across all their follow-up visits. Figure 2 (Right) shows that these outcomes (except WHR) are highly

correlated with each other.

Covariates

Mothers were interviewed for 2 hours during enrollment to gather covariate data. The computerized perinatal database at Mount Sinai Hospital was used to obtain pregnancy and delivery information. Gestational weight gain adequacy is calculated by dividing the observed gestational weight gain (last pregnancy weight minus self-reported pre-pregnancy weight) by the expected gestational weight gain based on the 2009 Institute of Medicine guidelines times 100 ([Institute of Medicine/National Research Council, 2009](#)). We categorize gestational weight gain as inadequate if the ratio is $< 86\%$, adequate if $86\% - 120\%$, and excessive if $> 120\%$. The final baseline covariates include the mother’s age, mother’s BMI, mother’s gestational weight gain adequacy category, mother’s smoking status, mother’s education, mother’s race, whether mother breastfed, child’s sex, child’s birth weight, and creatinine concentration. The children’s age in months was also recorded at each follow-up visit and included as a covariate.

3 Multivariate Bayesian factor regression with time-varying effects

3.1 Model correlated chemical mixtures with a latent factor model

Let X_i be a p -vector of correlated metabolite concentrations measured during the third trimester of pregnancy for subject i . We assume that variation in X_i can be attributed to $K < p$ latent variables:

$$X_i \sim N_p(\Theta\eta_i, \Sigma_X) \tag{1}$$

$$\eta_i \sim N_K(0, \mathbf{I}) \tag{2}$$

$$\Sigma_X = \text{diag}(\sigma_{X,1}^2, \dots, \sigma_{X,p}^2) \tag{3}$$

where η_i is a K -vector of unobserved latent factors of subject i , Θ is the factor loadings matrix, and $\sigma_{X,1}^2, \dots, \sigma_{X,p}^2$ are idiosyncratic noise variances. We assume the exposures have been mean-centered and remove the intercepts. Independent priors on each $\sigma_{X,1}^2 \dots \sigma_{X,p}^2$ are chosen to be those often used in factor analysis. We use the multiplicative gamma process (MGP) prior on the factor loadings to learn sparse loadings structure and infer the number of factors K ([Bhattacharya and Dunson, 2011b](#)):

$$\theta_{jk} \sim N(0, \phi_{jk}^{-1} \tau_k^{-1}) \quad (4)$$

$$\phi_{jk} \sim G(v/2, v/2), \quad j = 1, \dots, p; k = 1, \dots, K \quad (5)$$

$$\tau_h = \prod_{l=1}^h \delta_l, \quad \delta_1 \sim G(a_1, 1), \quad \delta_{l \geq 2} \sim G(a_2, 1) \quad (6)$$

3.2 Model correlated outcomes as a function of latent factors

Let $Y_{it} = (y_{it1}, \dots, y_{itq})^T$ be a vector of q outcomes at follow-up time $t = 1, \dots, T_i$, where T_i is the number of follow-ups with at least one measured outcome for subject i . We assume each outcome at each follow-up has been mean-centered and remove the intercepts. We also assume the variation in the outcomes Y_{it} can be decomposed into the variation explained by the latent factors of X_i , the variation due to unobserved factors and idiosyncratic noise:

$$Y_{it} \sim N_q(B(t)\eta_i + \xi_i, \Sigma_Y) \quad (7)$$

$$\xi_i \sim N_H(0, \nu^2 \Sigma_Y) \quad (8)$$

$$\Sigma_Y \sim IW(s_0, S_0) \quad (9)$$

where ν^2 has a half-t prior with a small degree of freedom for an uninformative prior that still behaves well in the case that ν^2 is close to zero, as suggested by [Gelman \(2006\)](#). Random variables ξ_i are subject-level random intercepts. Σ_Y is the residual covariance, which describes variances and covariances in the outcome due to unmeasured factors as well as random noise. We can interpret $\frac{\nu^2}{\nu^2+1}$ as the proportion of total residual variation explained by between-subject variation, and $\frac{1}{\nu^2+1}$ as the proportion of residual variation explained by within-subject variation.

3.3 Model health effects as flexible functions of time

B is a $(q \times K)$ matrix of regression functions, which is of primary interest to our analysis. Element jk in B models the effect of the k^{th} latent factor on the j^{th} outcome that can vary smoothly and flexibly over follow-up times. We consider Gaussian processes as priors to learn these smooth regression functions on a discrete-time grid $t = 1, \dots, T$, where T is the total number of unique ages at which children had follow-up visits. At the same time, we want to incorporate our belief that effects across adiposity outcomes, which are driven by similar mechanisms through which phthalates interfere with the body's hormones, should be correlated. As a result, instead of placing independent Gaussian process priors on elements of B , we adopt the following factorization:

$$B(t) = \Lambda U(t) \quad (10)$$

$$u_{hk} \sim GP(0, c_\kappa(t, t')), \quad c_\kappa(t, t') = e^{-\frac{1}{2}[\frac{(t-t')}{\kappa}]^2} \quad (11)$$

$$\lambda_{jh} \sim MGP, \quad j = 1, \dots, p; h = 1, \dots, H; k = 1, \dots, K \quad (12)$$

where Λ is a $q \times H$ matrix, with $H \leq K$, that linearly combines H independent basis functions into elements of B . A similar factorization was used by [Fox and Dunson \(2015\)](#), but their work focused on covariance regression. We also use the MGP prior on the basis functions loadings to learn sparse loadings structure and help infer the number of basis functions H ([Bhattacharya and Dunson, 2011b](#)). U is a matrix of independent basis functions. We choose the Gaussian kernel $c(t, t')$ for all elements of U to ensure the time-varying effects are smooth functions of time with the same wiggleness encoded in a shared length scale κ . Since the input is on a grid, we place a uniform prior on a grid of plausible values for κ . Conditional on Λ , the k^{th} column of B has a separable Gaussian process prior:

$$B_k \sim N_{q \times T}(0, \Lambda \Lambda^T, C) \quad (13)$$

where $\Lambda \Lambda^T$ describes the covariance in the regression functions of factor k across outcomes, and $C_{rs} = c_\kappa(t_r, t_s)$. Thus, $Cov(B_{jk}) = [\Lambda \Lambda^T]_{jj} C$, so we set the amplitude of the kernel to 1 for identifiability.

3.4 Model linear effects and interactions of covariates

Let Z_{it} be a L -vector of covariates, including both baseline covariates and those collected at follow-up time t . For covariates where the linear relationships are reasonable, we can add a linear effect term to equation (4) as follows:

$$Y_{it} \sim N_q(B(t)\eta_i + B^{(c)}Z_{it} + \xi_i, \Sigma_Y) \quad (14)$$

We endow the regression coefficient matrix $B^{(c)}$ with a global-local shrinkage prior on matrix normal parameters of [Bai and Ghosh \(2018\)](#):

$$\begin{aligned} B^{(c)} &\sim N_{q \times L}(0, \Sigma_Y, \Psi^{(c)}) \\ \Psi^{(c)} &= \text{diag}(\psi_1^{(c)}, \dots, \psi_L^{(c)}) \\ \psi_l^{(c)} | \zeta_l^{(c)} &\sim G(u, \zeta_l^{(c)}) \\ \zeta_l^{(c)} &\sim G(v, r) \end{aligned}$$

Shrinkage parameter $\psi_l^{(c)}$ provides variable selection to determine if predictor l is important to all outcomes, which fits our application. Outcome-specific effects within column l can additionally shrink toward zero. The authors in ([Bai and Ghosh, 2018](#)) suggested setting the global shrinkage parameter

$r = 1/(K\sqrt{n \ln n})$ to satisfy sufficient conditions for posterior consistency (Bai and Ghosh, 2018). When $u = v = 1/2$, this is the horseshoe prior (Armagan et al., 2011; Bai and Ghosh, 2018). A similar setup can be used for any linear interactions between the latent factors and covariates.

3.5 Imputation of censored and missing data

We have very few missing outcomes at recorded follow-up visits (2 missing FMP and 1 missing BMIz measurement out of 364 observations). In the case that it's reasonable to assume outcomes are missing at random conditional on observed covariates and birth weight data (Buckley et al., 2016b), we impute them during MCMC. We sample $Y_{it,mis}$ given $Y_{it,obs}$, ω from a conditional multivariate normal, where ω are all unknown parameters:

$$Y_{it,mis} | Y_{it,obs}, \omega \sim N(m, V) \quad (15)$$

$$m = B(t)_{mis} \eta_{i,mis} + \Sigma_{Y,mis,obs} \Sigma_{Y,obs,obs}^{-1} [Y_{it,obs} - B(t)_{obs} \eta_{i,obs}] \quad (16)$$

$$V = \Sigma_{Y,mis,mis} - \Sigma_{Y,mis,obs} \Sigma_{Y,obs,obs}^{-1} \Sigma_{Y,obs,mis} \quad (17)$$

where $B(t)_{mis}$, $\eta_{i,mis}$ are parameters corresponding to the indices of the missing values, $B(t)_{obs}$, $\eta_{i,obs}$ are parameters at observed indices, $\Sigma_{Y,mis,obs}$ is the covariances between missing and observed indices, $\Sigma_{Y,mis,mis}$ is the covariance matrix of missing indices, and $\Sigma_{Y,obs,obs}$ is the covariance matrix of observed indices.

Moreover, we often observe censored metabolite concentrations that are below the limit of detection (LOD). The LOD is defined as the lowest concentration of an analyte in a sample that can be reliably distinguished from the highest concentration of the same analyte in a sample with no such analyte (Armbruster and Pry, 2008). We can impute metabolite concentrations under the LOD by sampling from a conditional truncated normal at each MCMC iteration:

$$X_{ij} | X_{ij} \in \{-\infty, \log(LOD_j)\}, \omega \sim TN(\theta_j^T \eta_i, \sigma_{X,j}^2, -\infty, \log(LOD_j)) \quad (18)$$

where LOD_j is the LOD of the j^{th} chemical, θ_j is the j^{th} row of loading matrix Θ , and $TN(m, v, a, b)$ is a truncated normal distribution with mean m , variance v , and support $[a, b]$.

3.6 Posterior computation

See Appendix for full conditional and adaptive Metropolis-within-Gibbs updates.

4 Simulations

We compare our proposed method with the following approaches: 1) two-stage univariate regressions, 2) BVCKMR, and 3) a baseline mean model. In the two-stage approach, we reduce the dimension of the exposures using PCA, keeping the first few principal components (PCs), and then fit LMM for each outcome separately. The baseline mean model returns the mean of each outcome. We simulate data from the following three scenarios to demonstrate our method's utility compared to existing approaches. For all scenarios, we generate data for $n = 200$ subjects. We generate the exposures according to a factor model, creating correlated exposures with group structures, similar to the observed phthalates metabolites:

$$\begin{aligned} X_i &= \Theta \eta_i + e_i \quad \text{for } i = 1, \dots, n \\ \eta_i &\sim N_{K^*}(0, I), \quad e_i \sim N_p(0, I) \end{aligned}$$

We generate sparse Θ so that every five metabolites load onto one factor for $p = 10$ and $K^* = 2$ latent factors. The non-zero entries of Θ are sampled from $N(0, 1)$. We generate $q = 5$ outcomes measured at $T_i = 10$ time points for all subjects:

$$\begin{aligned} Y_{it} &= \mathbf{g}(X_i, t) + \xi_i + \epsilon_{it} \\ \xi_i &\sim N_q(0, C_\xi), \quad \epsilon_{it} \sim N_q(0, C_\epsilon) \end{aligned}$$

We use different exposure-response functions \mathbf{g} including time-varying effects, different distributions for the random intercept ξ_i and random error ϵ_{it} for each scenario. Below is the description of each simulation scenario:

1. Linear exposure-response function where the first two factors are important, independent responses:

$$\begin{aligned} \mathbf{g}(X, t) &= \mathbf{h}(\eta, t) = \beta_1^T \eta + \beta_2^T \eta t, \quad j = 1, \dots, 10; k = 1, \dots, K^* \\ \beta_{1jk} &\sim U(-3, 3), \quad \beta_{2jk} \sim U(-0.5, 0.5) \\ C_\xi &= I, \quad C_\epsilon = 0.5I \end{aligned}$$

where \mathbf{h} is the latent factor-response function. The induced effects of X range from 0 to 1. Under this setting, all assumptions for PCA-LMM are satisfied, though it does not propagate the uncertainty from the first stage.

2. Non-linear time-varying exposure-response function where the first two factors are important, positively correlated responses:

$$\begin{aligned} \mathbf{g}(X, t) &= \mathbf{h}(\eta, t) = [\beta u(t)^T] \eta \\ u_1(t) &= 3.5/(1 + \exp(-3t + 25)), \quad u_2(t) = 9 \text{dnorm}((t - 5.5)/1.5) \\ \beta &\sim N_q(0, I) \end{aligned}$$

where $dnorm(t)$ is the standard normal pdf at t . Covariances C_ξ and C_ϵ have composite symmetry structure with high correlation of 0.7. Under this setting, all assumptions for our model are satisfied.

3. Quadratic exposure-response function where 3 metabolites are important, responses are independent:

$$\begin{aligned} \mathbf{g}(X, t) &= \beta_1 X_1^2 - \beta_2 X_6^2 + 0.5\beta_3 X_1 X_2 + \beta_4 X_7 + \beta_5 X_8 + 0.3(\beta_6 X_1^2 + \beta_7 X_7 + \beta_8 X_8)t \\ \beta_{lj} &\sim Unif(0.25, 0.5) \bigcup Unif(-0.5, 0.25), \quad l = 1, \dots, 8 \\ C_\xi &= I, \quad C_\epsilon = 0.5I \end{aligned}$$

This scenario is most favorable for BVCKMR.

We choose $K = K^* + 2$ for PCA and our method, and $H = 2$ for our method, to resemble analyses where K, H are close to but not exactly the true latent dimension. For predictive performance evaluation, we calculate the mean predictive square error (MPSE) on a test set of 200 subjects at 10 time points. Additionally, to evaluate how well the methods measure the relative importance of each chemical, we calculate the Spearman correlation between the true relative importance rank and the inferred rank of chemicals in X . The rank is based on the absolute value of the effect at each time point, summed over all time points. We calculate the rank for our model by first calculating the induced effects in the original predictors X at each time point as shown in [Ferrari and Dunson \(2021\)](#). Similarly, we can calculate the effects from the PCA-LMM analysis in X as $\hat{\beta}_X = V^{(K)} \hat{\beta}_{PCs}$, where $V^{(K)}$ is the first K left singular vectors, and $\hat{\beta}_{PCs}$ is a vector of regression coefficients for the PCs. Table 1 shows the MPSE results. Note that PCA-LMM performed worst in all scenarios, even when all its assumptions were met. Our method performs best when the data are generated according to its model. When the data are more favorable to the other models, our method still outperforms PCA-LMM. Table 2 shows the Spearman correlation results. Here, our method performs best in the first two scenarios and is very close to the best in the third scenario.

Table 1: Average MPSE of 100 simulations per scenario.

	scenario 1	scenario 2	scenario 3
Oracle	1.51 (0.05)	1.51 (0.08)	1.30 (0.02)
Mean predictor	12.0 (2.65)	7.57 (4.6)	3.93 (0.25)
PCA-LMM	7.14 (1.95)	5.93 (2.81)	3.23 (0.28)
BVCKMR	4.44 (1.17)	5.69 (2.55)	1.60 (0.04)
Our model	5.33 (1.46)	2.92 (1.31)	2.63 (0.22)

Table 2: Average Spearman’s correlation of rank of variable importance of 100 simulations per scenario.

	scenario 1	scenario 2	scenario 3
Oracle	1	1	1
Mean predictor	-	-	-
PCA-LMM	0.81 (0.07)	0.63 (0.22)	0.29 (0.14)
BVCKMR	0.76 (0.08)	0.54 (0.19)	0.59 (0.1)
Our model	0.89 (0.06)	0.89 (0.08)	0.55 (0.17)

5 Analysis of Mount Sinai birth cohort data

5.1 Data preprocessing

We log-transformed WC so that its marginal is more approximately normal. We mean-centered all outcomes. We also used the logarithm of phthalate metabolites as exposures. We corrected for urinary dilution by dividing the metabolite concentrations (not on the log scale) by the Cratio as discussed in Section 2. We standardize other continuous covariates and create dummy variables for categorical covariates. We used R package `mice` for multiple imputation of missing values in the covariates. We created a time variable that is age in years based on age in months of the children at follow-up visits. Age ranges from 4 to 10 years old (Figure 3).

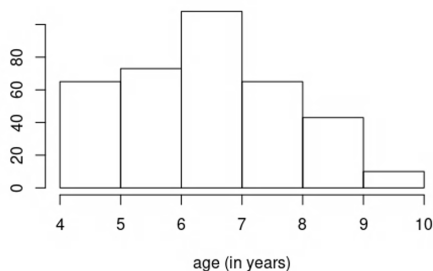


Figure 3: Histogram of ages at which the children had adiposity outcomes’ measurements.

5.2 Preliminary analysis

As a preliminary analysis, we did two-staged PCA-LMM analyses of each of the four outcomes. We applied PCA to the standardized log chemical exposures. We used the first three principal components (PCs) for the LMM stage because they explained over 90% of the variations in the exposures. The first three PCs can be interpreted as the non-DEHP (excluding MEP) factor, DEHP factor, and MEP factor respectively. The PCA factor loading matrix is available in Appendix 7, Section 7.2.

We fitted four independent LMMs for four outcomes with random intercepts and interactions between the PCs and the child’s gender, controlling for all baseline covariates. We fitted a second set of LMMs with interactions between the PCs, child’s gender, and child’s age, and a third set with interactions between the PCs, child’s gender, and polynomials of degree 2 of child’s age. We used AIC, BIC, likelihood ratio tests, and 6-fold cross-validated MPSE for model comparison within each outcome. After Bonferroni correction for multiple testing, we still saw evidence from the likelihood ratio tests that models with linear interactions with age were the best fits for FMP, WHR, and WC. Models with linear interactions with age had the best cross-validated MPSE for BMIz, FMP, and WC. We saw insufficient evidence of the quadratic interactions in age being useful. Full summary tables of AIC, BIC, p-values, and MPSEs can be found in Appendix 7, Section 7.2.

5.3 Analysis via our model

In the main analysis, we fitted our proposed Bayesian multivariate factor regression with time-varying effects to all four outcomes simultaneously. We fitted two models, one for male and one for female children, to assess any sex-specific effects. We controlled for linear main effects of covariates and included random intercepts.

We used the following prior specifications. Since we standardized the log chemical exposures to have unit variances, we set hyperparameters for inverse gamma priors on idiosyncratic noise variances $\sigma_{X,1}^2, \dots, \sigma_{X,H}^2$ so that they are less than 1 with 99% probability. For hyperparameters on the MGP prior for loadings Θ and Λ , we used $a_1 = 2.1$ and $a_2 = 3.1$ as suggested in the note by Durante (2017). For the IW prior on Σ_Y , we set S_0 to the sample covariance of the four outcomes, and a small $s_0 = 6$ so that prior is loosely centered around the sample covariance. For a weakly informative prior that ν^2 should be below 100, we use a half-Cauchy with a scale of 25 as done in Gelman (2006).

We selected the number of factors K and the number of basis functions H using grid search. We chose the combination of K and H from a set of options ($K \in \{2, 3, 4\}$, and $H \in \{1, 2\}$) that had the smallest 6-fold cross-validated MPSE, with $H \leq K$ only. We considered small values for H because of our prior belief that the effects of the exposures on all outcomes were similar. The final model for males had $K = 3, H = 1$; and the one for females had $K = 3, H = 2$. We fixed the length scale parameter $\kappa = 6$, since we observed from our preliminary analysis that there were likely no highly variable effects. Sensitivity analysis was also done for models that infer the length scale parameter during MCMC.

5.4 Results of analysis via our model

For out-of-sample predictive performance comparison, we calculated MPSE of a baseline mean model that returned outcome-specific means. The 6-fold cross-validated MPSE of our proposed method is 0.93 compared to 0.98 of the baseline

mean model. For the female model, our proposed method’s MPSE is 0.82 compared to 1.04 of the baseline mean model. On the whole data set (combining male and female), our MPSE is 0.88, compared to 0.92 of PCA-LMMs with linear interactions with age, and 1.03 of the baseline mean model.

For interpretation of the results, we resolved rotational and label-switching ambiguity in the factors using the MatchAlign algorithm proposed by [Poworoznek et al. \(2021\)](#). Figure 4 shows the post-processed factor loading matrix and time-varying effects of each latent factor from the model fitted for male children. Time-varying effects were transformed to represent the effects of one unit increase in the latent factors. We identified two main latent factors corresponding to the non-DEHP group and DEHP group of chemicals. This is consistent with previous studies on phthalate ([Maresca et al., 2016](#)). Though both groups of chemicals seem to be associated with lower values in adiposity outcomes at younger ages, their promotive effects of obesity seem to increase over time. The latent factors identified in the model for female also includes non-DEHP and DEHP groups, though all effects seem to remain null over time (Figure 5). The sex-specific effects here could be related to phthalates being anti-androgens ([Fisher, 2004](#)). Though the C.I.s from the female model are not statistically significant, the effects of latent factors on WHR seem to be different from their effects on the other three outcomes. This could be related to the fact that WHR is less correlated to the other outcomes than they are to each other.

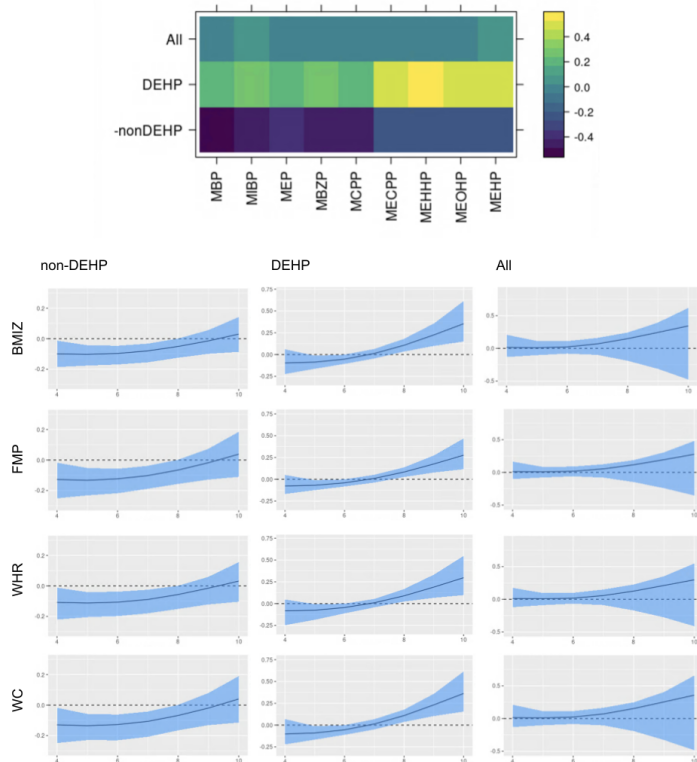


Figure 4: MatchAligned factor loading matrix and time-varying effects of each latent factor from the model fitted for males. The blue band displays 95% posterior credible interval, and the black solid line shows the posterior mean.

We included results from sensitivity analysis of inferring the length scale parameter during MCMC in Appendix 7, Section 7.2. Overall, the sensitivity analysis results were similar to results in Figure 4 and Figure 5.

6 Discussion

This paper presents a Bayesian multivariate factor regression to assess the health effects of correlated chemical mixtures on a set of multivariate adiposity outcomes measured in young children over time. It adds to the literature by allowing flexible interrogation of multivariate outcomes measured longitudinally when exposures are correlated environmental mixtures. Missing data, including exposures below a limit of detection, are imputed as part of the MCMC algorithm. The sharing of information across multiple longitudinal outcomes

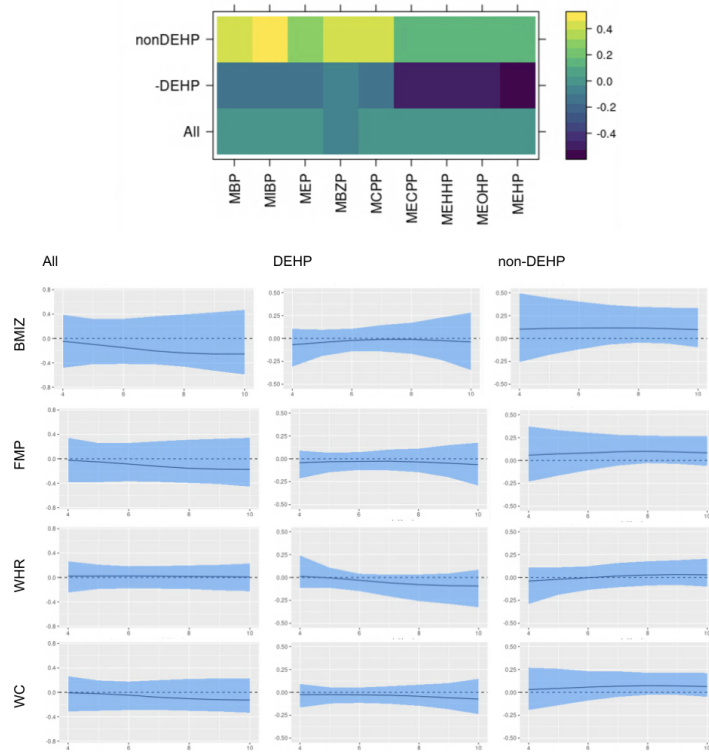


Figure 5: MatchAligned factor loading matrix and time-varying effects of each latent factor from the model fitted for females. The blue band displays 95% posterior credible interval, and the black solid line shows the posterior mean.

improves efficiency over one-at-a-time regression models. We use Gaussian process priors on the regression coefficients to let them vary smoothly in time. We apply the model to the MSCEHS data and identify potential time-varying effects of phthalates on BMI z-score, fat mass percentage, waist-to-hip ratio, and waist circumference. Specifically, we found the associations between prenatal phthalate exposures and adiposity outcomes in male children to be negative at early ages but to become positive as the children get older. Our finding is consistent with previous longitudinal studies that also found somewhat positive associations between prenatal phthalate exposures and adiposity outcomes throughout childhood (Agay-Shay et al., 2015; Buckley et al., 2016a; Botton et al., 2016; Bowman et al., 2019; Ferguson et al., 2022; Gao et al., 2022; Güil-Oumrait et al., 2022; Kupsco et al., 2022), or a pattern of negative associations with BMI at early ages followed by positive associations at later ages (Sol et al., 2025).

7 Appendix

7.1 MCMC Algorithm

Let X be an $n \times p$ matrix of mixtures data, Y_{it} be a vector of q outcomes at time t for subject i , K be a bound on the number of latent factors,

1. Sample idiosyncratic noise variances for the mixtures Σ_X :

$$\sigma_{X,j}^{-2} | \cdot \sim G\left(\frac{2.5 + n}{2}, \frac{2.5(0.084) + \sum_{i=1}^n (X_{ij} - \theta_j^T \eta_i)^2}{2}\right)$$

where θ_j is the j^{th} row of loading matrix Θ , for $j = 1, \dots, p$. We use prior $\sigma_{X,j}^{-2} \sim G(\frac{2.5}{2}, \frac{2.5(0.084)}{2})$ since columns of X have been standardized to have variance 1.

2. Sample the mixtures loading matrix Θ :

$$\theta_j | \cdot \sim N_K\left(\left(D_j^{-1} + \frac{\eta^T \eta}{\sigma_{X,j}^2}\right)^{-1} \frac{\eta^T X_{\cdot j}}{\sigma_{X,j}^2}, \left(D_j^{-1} + \frac{\eta^T \eta}{\sigma_{X,j}^2}\right)^{-1}\right)$$

where $X_{\cdot j}$ is the j^{th} column of X , θ_j is the j^{th} row of Θ .

$$\phi_{jk} | \cdot \sim G\left(\frac{v+1}{2}, \frac{v + \tau_k \theta_{jk}^2}{2}\right)$$

for $k = 1, \dots, K$ and $v = 3$ as suggested in (Bhattacharya and Dunson, 2011a).

$$\delta_1 | \cdot \sim G\left(a_1 + \frac{pK}{2}, 1 + \frac{1}{2} \sum_{l=1}^K \tau_l^{(1)} \sum_{j=1}^p \phi_{jl} \theta_{jl}^2\right)$$

$$\delta_k | \cdot \sim G\left(a_2 + \frac{p(K-k+1)}{2}, 1 + \frac{1}{2} \sum_{l=1}^K \tau_l^{(k)} \sum_{j=1}^p \phi_{jl} \theta_{jl}^2\right)$$

for $k \geq 2$, where $\tau_l^{(k)} = \prod_{t=1, t \neq k}^l \delta_t$, for $k = 1, \dots, K$.

Set $\tau_k = \prod_{t=1}^k \delta_t$.

We set $a_1 = 2.1$ and $a_2 = 3.1$ following the note by (Durante, 2017).

3. Sample latent factors for each subject using adaptive Metropolis-within-Gibbs:

Sample a proposal $\eta_i^* \sim N(\eta_i^{(s)}, \tilde{s}_i^{(s)})$, where $\eta_i^{(s)}$ is the value for subject i at iteration s .

The log posterior density at η_i (after integrating out ξ_i) is proportional to:

$$\begin{aligned}
l(\eta_i) &= l_{X_i}(\eta_i) + l_\eta(\eta_i) + \sum_t^{T_i} l_{Y_{it}}(\eta_i) \\
l_{X_i}(\eta_i) &= -\frac{1}{2}\eta_i^T \Theta^T \Sigma_X^{-1} \Theta \eta_i; \quad l_\eta(\eta_i) = -\frac{1}{2}\eta_i^T \eta_i \\
l_{Y_{it}}(\eta_i) &= -\frac{1}{2}(1 + \nu^2)^{-1} m_{it}(\eta_i)^T \Sigma_Y^{-1} m_{it}(\eta_i) \\
m_{it}(\eta_i) &= Y_{it} - (B(t)\eta_i + \sum_l z_{itl} B_l^{(in)} \eta_i + B^{(c)} Z_{it})
\end{aligned}$$

With probability $\min(1, \exp\{l(\eta_i^*) - l(\eta_i^{(s)})\})$, accept the proposal and set $\eta_i^{(s+1)} = \eta_i^*$. Otherwise, set $\eta_i^{(s+1)} = \eta_i^{(s)}$.

Update the proposal scaling $\tilde{s}_i^{(s)}$ every 50 iterations according to Chapter 4, section 4.3 in (Brooks et al., 2011).

4. Sample subject-level random effects:

$$\xi_i | \cdot \sim N\left(\left(\frac{1}{\nu^2} + T_i\right)^{-1} \sum_t^{T_i} \tilde{Y}_{it}, \left(\frac{1}{\nu^2} + T_i\right)^{-1} \Sigma_Y\right)$$

for $i = 1, \dots, n$, where T_i is the number of follow-up times of subject i , and $\tilde{Y}_{it} = Y_{it} - B(t)\eta_i - \sum_l z_{itl} B_l^{(in)} \eta_i - B^{(c)} Z_{it}$.

Sample $\nu^2 | \cdot$ using Metropolis Hasting.

5. Sample basis function loading matrix Λ :

$$\begin{aligned}
\lambda_{.h} | \cdot &\sim N_q(V_{.h} m_{.h}, V_{.h}) \\
m_{.h} &= \sum_{i,t} u_{h.}(t)^T \eta_i Y_{it} \\
V_{.h} &= \left[D_h^{-1} + \Sigma^{-1} \left(\sum_{i,t} u_{h.}(t)^T \eta_i \right)^2 \right]^{-1}
\end{aligned}$$

where $D_h = \tau_h^* \text{diag}(\phi_{1h}^*, \dots, \phi_{qh}^*)$ contains MGP shrinkage parameters. Sample these the same as in Step 2.

6. Sample basis functions $U(t)$:

$$\begin{aligned}
D_i^{(hk)} &= \begin{bmatrix} \lambda_{.h}\eta_{ik}O_{i1} & \dots & 0 \\ 0 & \dots & 0 \\ 0 & \dots & \lambda_{.h}\eta_{ik}O_{iT} \end{bmatrix} \\
v_{it}^{(hk)} &= \begin{bmatrix} \sum_{l \neq h} \lambda_{1l}\eta_{ik}u(t)_{lk} \\ \dots \\ \sum_{l \neq h} \lambda_{ql}\eta_{ik}u(t)_{lk} \end{bmatrix} \\
v_i^{(hk)} &= \begin{bmatrix} v_{i1}^{(hk)} \\ \dots \\ v_{iT}^{(hk)} \end{bmatrix} \\
u^{(hk)} &\sim N(V^{(hk)}m^{(hk)}, V^{(hk)}) \\
V^{(hk)} &= \left[C^{-1} + \sum_i (D_i^{(hk)})^T \Sigma^{-1} D_i^{(hk)} \right]^{-1} \\
m^{(hk)} &= \sum_i (D_i^{(hk)})^T \Sigma^{-1} (y_i^{(k)} - v_i^{(hk)})
\end{aligned}$$

7. Sample Gaussian Process bandwidth κ from a set of plausible values:

Sample one option κ^* w.p. $\frac{l(\kappa^*; U)}{\sum l(\tilde{\kappa}; U)}$ where $l(\kappa^*; U)$ is the likelihood of κ^* .

8. Sample matrix of main effects of covariates:

$$B^{(c)}|. \sim N_{q \times L} \left(\frac{\tilde{Y}^T Z}{1 + \nu^2} \left(\frac{Z^T Z}{1 + \nu^2} + \Psi^{(c)-1} \right)^{-1}, \Sigma_Y, \left(\frac{Z^T Z}{1 + \nu^2} + \Psi^{(c)-1} \right)^{-1} \right)$$

where $\tilde{Y} = [\tilde{Y}_{11}, \dots, \tilde{Y}_{1T_1}, \dots, \tilde{Y}_{nT_n}]^T$ is an $\sum_i T_i \times q$ matrix, and $\tilde{Y}_{it} = Y_{it} - B(t)\eta_i - \sum_l^L z_{itl} B_l^{(in)} \eta_i$. Sample shrinkage parameters for the linear regression coefficient matrix $B^{(c)}$:

$$\begin{aligned}
\psi_l^{(c)}|. &\sim GIG\left(u - \frac{q}{2}, 2\zeta_l^{(c)}, B_l^{(c)T} \Sigma^{-1} B_l^{(c)}\right) \\
\zeta_l^{(c)}|. &\sim G(v, r + \psi_k^{(c)})
\end{aligned}$$

where $B_l^{(c)}$ is the l^{th} column of $B^{(c)}$, for $l = 1, \dots, L$.

9. Sample the outcomes' noise variance parameters:

$$\begin{aligned}
\Sigma|. &\sim IW\left(\sum_i^n T_i + KT + KL + L + s_0, SS + s_1 I_q\right) \\
SS &= Y^\dagger Y^{\dagger T} (1 + \nu^2)^{-1} + \sum_k^K B_k (\psi_k C)^{-1} B_k^T \\
&\quad + \sum_l^L B_l^{(in)} \Psi^{(in)-1} B_l^{(in)T} + B^{(c)} \Psi^{(c)-1} B^{(c)T}
\end{aligned}$$

where $Y^\dagger = [Y_{11}^\dagger, \dots, Y_{1T_1}^\dagger, \dots, Y_{nT_n}^\dagger]$ is a $q \times \sum_i^n T_i$ matrix, and $Y_{it}^\dagger = Y_{it} - B(t)\eta_i - \sum_l^L z_{itl}B_l^{(in)}\eta_i - B^{(c)}Z_{it}$.

We use the following parametrization of generalized inverse Gaussian $y \sim GIG(p, a, b)$ if $p(y) \propto y^{p-1}e^{-(ay+b/y)/2}$ for $y > 0$.

7.2 Analysis of Mount Sinai birth cohort data

7.2.1 Preliminary analysis

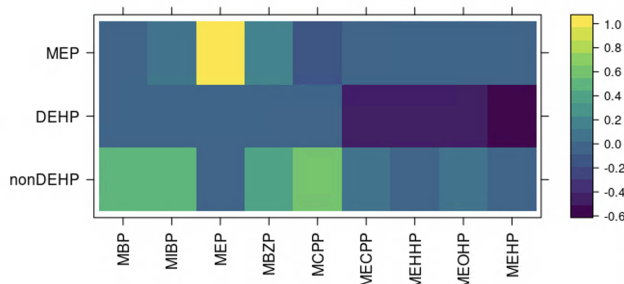


Figure 6: PCA varimax factor loading matrix of phthalate metabolites

Table 3: Model comparison for including none, linear, or polynomial degree 2 interactions with time to predict BMIz.

	AIC	BIC	Chisq	p-value	MPSE
none	727.	809	-	-	1.05
linear	736	845	4.87	0.67	1.03
quadratic	747	883	3.24	0.86	1.13

Table 4: Model comparison for including none, linear, or polynomial degree 2 interactions with time to predict FMP.

	AIC	BIC	Chisq	p-value	MPSE
none	859	941	-	-	1.03
linear	743	852	130	$< 2e - 16$	0.90
quadratic	749	885	8	0.33	1.32

Table 5: Model comparison for including none, linear, or polynomial degree 2 interactions with time to predict WHR.

	AIC	BIC	Chisq	p-value	MPSE
none	1004	1086	-	-	0.94
linear	988	1097	30	$7e - 5$	0.98
quadratic	986	1123	15	0.03	2.61

Table 6: Model comparison for including none, linear, or polynomial degree 2 interactions with time to predict WC.

	AIC	BIC	Chisq	p-value	MPSE
none	939	1021	-	-	1.1
linear	752	861	201	$< 2e - 16$	0.80
quadratic	761	898	4.4	0.73	1.73

7.2.2 Sensitivity analysis

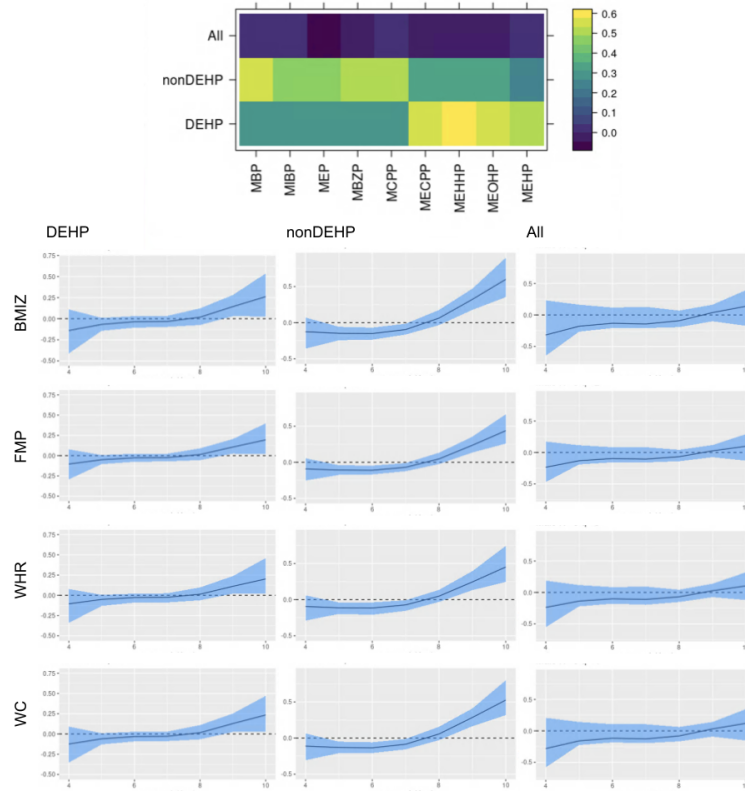


Figure 7: MatchAligned factor loading matrix and time-varying effects of each latent factor from the model fitted for male with an inferred κ .

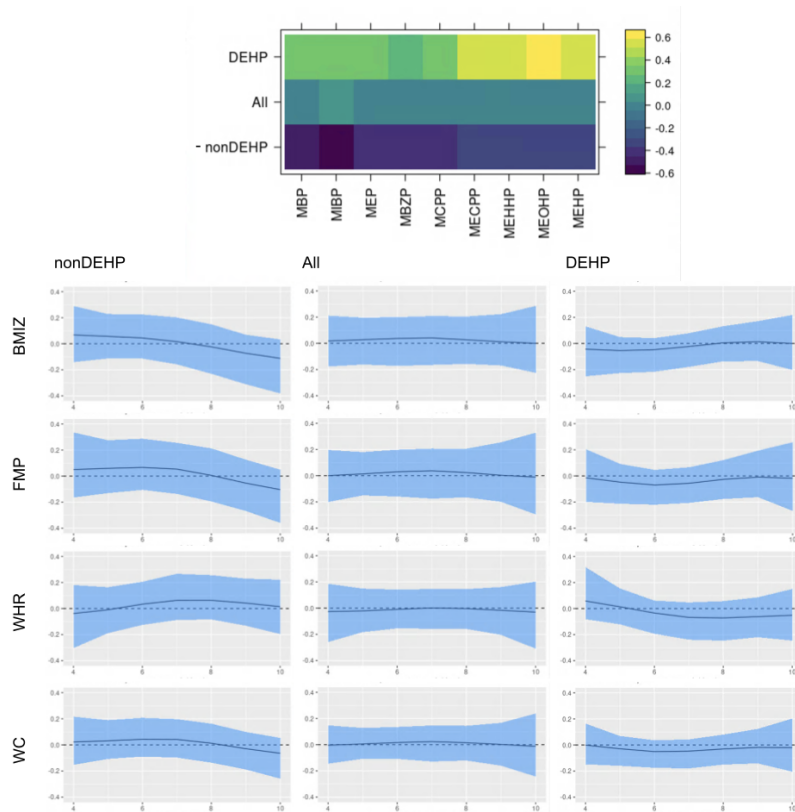


Figure 8: MatchAligned factor loading matrix and time-varying effects of each latent factor from the model fitted for females with an inferred κ .

References

- K. Agay-Shay, D. Martinez, D. Valvi, R. Garcia-Esteban, X. Basagaña, O. Robinson, M. Casas, J. Sunyer, and M. Vrijheid. Exposure to endocrine-disrupting chemicals during pregnancy and weight at 7 years of age: a multi-pollutant approach. *Environmental health perspectives*, 123(10):1030–1037, 2015.
- A. Armagan, D. B. Dunson, and M. Clyde. Generalized beta mixtures of gaussians. *Advances in neural information processing systems*, 24:523–531, 2011.
- D. A. Armbruster and T. Pry. Limit of blank, limit of detection and limit of quantitation. *The clinical biochemist reviews*, 29(Suppl 1):S49, 2008.

- R. Bai and M. Ghosh. High-dimensional multivariate posterior consistency under global-local shrinkage priors. *Journal of Multivariate Analysis*, 167:157–170, 2018.
- K. Berger, C. Hyland, J. L. Ames, A. M. Mora, K. Huen, B. Eskenazi, N. Holland, and K. G. Harley. Prenatal exposure to mixtures of phthalates, parabens, and other phenols and obesity in five-year-olds in the chamacos cohort. *International journal of environmental research and public health*, 18(4):1796, 2021.
- A. Bhattacharya and D. B. Dunson. Sparse bayesian infinite factor models. *Biometrika*, 98(2):291–306, 2011a.
- A. Bhattacharya and D. B. Dunson. Sparse bayesian infinite factor models. *Biometrika*, 98(2):291–306, 2011b. URL <https://doi.org/10.1093/biomet/asr013>.
- J. F. Bobb, L. Valeri, B. Claus Henn, D. C. Christiani, R. O. Wright, M. Mazumdar, J. J. Godleski, and B. A. Coull. Bayesian kernel machine regression for estimating the health effects of multi-pollutant mixtures. *Biostatistics*, 16(3):493–508, 2015.
- J. Botton, C. Philippat, A. M. Calafat, S. Carles, M.-A. Charles, R. Slama, E. M.-C. C. S. Group, et al. Phthalate pregnancy exposure and male offspring growth from the intra-uterine period to five years of age. *Environmental research*, 151:601–609, 2016.
- A. Bowman, K. E. Peterson, D. C. Dolinoy, J. D. Meeker, B. N. Sánchez, A. Mercado-Garcia, M. M. Téllez-Rojo, and J. M. Goodrich. Phthalate exposures, dna methylation and adiposity in mexican children through adolescence. *Frontiers in Public Health*, 7:162, 2019.
- S. Brooks, A. Gelman, G. Jones, and X.-L. Meng. *Handbook of markov chain monte carlo*. CRC press, 2011.
- J. P. Buckley, S. M. Engel, J. M. Braun, R. M. Whyatt, J. L. Daniels, M. A. Mendez, D. B. Richardson, Y. Xu, A. M. Calafat, M. S. Wolff, et al. Prenatal phthalate exposures and body mass index among 4 to 7 year old children: A pooled analysis. *Epidemiology (Cambridge, Mass.)*, 27(3):449, 2016a.
- J. P. Buckley, S. M. Engel, M. A. Mendez, D. B. Richardson, J. L. Daniels, A. M. Calafat, M. S. Wolff, and A. H. Herring. Prenatal phthalate exposures and childhood fat mass in a new york city cohort. *Environmental health perspectives*, 124(4):507–513, 2016b.
- M. C. Buser, H. E. Murray, and F. Scinicariello. Age and sex differences in childhood and adulthood obesity association with phthalates: analyses of nhanes 2007–2010. *International journal of hygiene and environmental health*, 217(6):687–694, 2014.

- CDC. A SAS program for the cdc growth charts (ages 0 to < 20 years). <https://www.cdc.gov/nccdphp/dnpao/growthcharts/resources/sas.htm>, 2004. Accessed: 2013-01-07.
- CDC. Updated tables, february 2012 what's new and different? https://www.cdc.gov/exposurereport/pdf/archives/ExposureReport_WND_Feb2012.pdf, 2012. Accessed: 2015-04-01.
- E. Colicino, K. Margetaki, D. Valvi, N. F. Pedretti, N. Stratakis, M. Vafeiadi, T. Roumeliotaki, S. A. Kyrtopoulos, H. Kiviranta, E. G. Stephanou, et al. Prenatal exposure to multiple organochlorine compounds and childhood body mass index. *Environmental Epidemiology*, 6(3), 2022.
- Committee on Accelerating Progress in Obesity Prevention and others. *Accelerating progress in obesity prevention: solving the weight of the nation*. National Academies Press, 2012.
- D. Durante. A note on the multiplicative gamma process. *Statistics & Probability Letters*, 122:198–204, 2017.
- S. M. Engel, G. S. Berkowitz, D. B. Barr, S. L. Teitelbaum, J. Siskind, S. J. Meisel, J. G. Wetmur, and M. S. Wolff. Prenatal organophosphate metabolite and organochlorine levels and performance on the brazelton neonatal behavioral assessment scale in a multiethnic pregnancy cohort. *American journal of epidemiology*, 165(12):1397–1404, 2007.
- K. K. Ferguson, P. A. Bommarito, O. Arogbokun, E. M. Rosen, A. P. Keil, S. Zhao, E. S. Barrett, R. H. Nguyen, N. R. Bush, L. Trasande, et al. Prenatal phthalate exposure and child weight and adiposity from in utero to 6 years of age. *Environmental health perspectives*, 130(4):047006, 2022.
- F. Ferrari and D. B. Dunson. Bayesian factor analysis for inference on interactions. *Journal of the American Statistical Association*, 116(535):1521–1532, 2021.
- J. S. Fisher. Environmental anti-androgens and male reproductive health: focus on phthalates and testicular dysgenesis syndrome. *Reproduction*, 127(3):305–315, 2004.
- E. B. Fox and D. B. Dunson. Bayesian nonparametric covariance regression. *The Journal of Machine Learning Research*, 16(1):2501–2542, 2015.
- C. Fryar, M. Carroll, and J. Afful. Prevalence of overweight, obesity, and severe obesity among children and adolescents aged 2–19 years: United states, 1963–1965 through 2017–2018. *NCHS Health E-Stats*, 2020.
- H. Gao, M.-l. Geng, H. Gan, K. Huang, C. Zhang, B.-b. Zhu, L. Sun, X. Wu, P. Zhu, F.-b. Tao, et al. Prenatal single and combined exposure to phthalates associated with girls' bmi trajectory in the first six years. *Ecotoxicology and Environmental Safety*, 241:113837, 2022.

- A. Gelman. Prior distributions for variance parameters in hierarchical models (comment on article by browne and draper). 2006.
- M. Golestanzadeh, R. Riahi, and R. Kelishadi. Association of exposure to phthalates with cardiometabolic risk factors in children and adolescents: a systematic review and meta-analysis. *Environmental Science and Pollution Research*, 26:35670–35686, 2019.
- S. E. Gollust, J. Niederdeppe, and C. L. Barry. Framing the consequences of childhood obesity to increase public support for obesity prevention policy. *American journal of public health*, 103(11):e96–e102, 2013.
- N. Güül-Oumrait, G. Cano-Sancho, P. Montazeri, N. Stratakis, C. Warembourg, M.-J. Lopez-Espinosa, J. Vioque, L. Santa-Marina, A. Jimeno-Romero, R. Ventura, et al. Prenatal exposure to mixtures of phthalates and phenols and body mass index and blood pressure in spanish preadolescents. *Environment International*, 169:107527, 2022.
- M. Haddouchi and A. Berrado. A survey of methods and tools used for interpreting random forest. In *2019 1st International Conference on Smart Systems and Data Science (ICSSD)*, pages 1–6. IEEE, 2019.
- K. G. Harley, K. Berger, S. Rauch, K. Kogut, B. Claus Henn, A. M. Calafat, K. Huen, B. Eskenazi, and N. Holland. Association of prenatal urinary phthalate metabolite concentrations and childhood bmi and obesity. *Pediatric research*, 82(3):405–415, 2017.
- B. C. Heggeseth, N. Holland, B. Eskenazi, K. Kogut, and K. G. Harley. Heterogeneity in childhood body mass trajectories in relation to prenatal phthalate exposure. *Environmental research*, 175:22–33, 2019.
- C. G. Howe, K. Margetaki, M. Vafeiadi, T. Roumeliotaki, M. Karachaliou, M. Kogevas, R. McConnell, S. P. Eckel, D. V. Conti, M. Kippler, et al. Prenatal metal mixtures and child blood pressure in the rhea mother-child cohort in greece. *Environmental Health*, 20(1):1–16, 2021.
- Institute of Medicine/National Research Council. Weight gain during pregnancy: Reexamining the guidelines (rasmussen km, yaktine al, eds). Technical report, 2009.
- T. Jung and K. A. Wickrama. An introduction to latent class growth analysis and growth mixture modeling. *Social and personality psychology compass*, 2(1):302–317, 2008.
- S. Kim and M. Park. Phthalate exposure and childhood obesity. *Ann Pediatr Endocrinol Metab*, 19(2):69–75, 2014.
- A. Kupsco, H. Wu, A. M. Calafat, M.-A. Kioumourtzoglou, A. Cantoral, M. Tamayo-Ortiz, I. Pantic, M. L. Pizano-Zárate, E. Oken, J. M. Braun, et al. Prenatal maternal phthalate exposures and trajectories of childhood

- adiposity from four to twelve years. *Environmental research*, 204:112111, 2022.
- S. H. Liu, J. F. Bobb, B. Claus Henn, C. Gennings, L. Schnaas, M. Tellez-Rojo, D. Bellinger, M. Arora, R. O. Wright, and B. A. Coull. Bayesian varying coefficient kernel machine regression to assess neurodevelopmental trajectories associated with exposure to complex mixtures. *Statistics in medicine*, 37(30):4680–4694, 2018.
- M. M. Maresca, L. A. Hoepner, A. Hassoun, S. E. Oberfield, S. J. Mooney, A. M. Calafat, J. Ramirez, G. Freyer, F. P. Perera, R. M. Whyatt, et al. Prenatal exposure to phthalates and childhood body size in an urban cohort. *Environmental health perspectives*, 124(4):514–520, 2016.
- K. V. Narayan, J. P. Boyle, T. J. Thompson, S. W. Sorensen, and D. F. Williamson. Lifetime risk for diabetes mellitus in the united states. *Jama*, 290(14):1884–1890, 2003.
- National Academies of Sciences, Engineering, and Medicine and others. The interplay between environmental chemical exposures and obesity: proceedings of a workshop. 2016.
- K. M. O’Brien, K. Upson, and J. P. Buckley. Lipid and creatinine adjustment to evaluate health effects of environmental exposures. *Current environmental health reports*, 4:44–50, 2017.
- E. Poworoznek, F. Ferrari, and D. Dunson. Efficiently resolving rotational ambiguity in bayesian matrix sampling with matching. *arXiv preprint arXiv:2107.13783*, 2021.
- M. Y. Seo, S. Moon, S.-H. Kim, and M. J. Park. Associations of phthalate metabolites and bisphenol a levels with obesity in children: The korean national environmental health survey (konehs) 2015 to 2017. *Endocrinology and Metabolism*, 37(2):249–260, 2022.
- C. M. Sol, G. Delgado, K. Kannan, V. W. Jaddoe, L. Trasande, and S. Santos. Fetal exposure to phthalates and body mass index from infancy to adolescence. the generation r study. *Environmental Research*, 274:121253, 2025.
- L. Trasande, T. M. Attina, S. Sathyanarayana, A. J. Spanier, and J. Blustein. Race/ethnicity-specific associations of urinary phthalates with childhood body mass in a nationally representative sample. *Environmental health perspectives*, 121(4):501–506, 2013.
- M. Vafeiadi, A. Myridakis, T. Roumeliotaki, K. Margetaki, G. Chalkiadaki, E. Dermitzaki, M. Venihaki, K. Sarri, M. Vassilaki, V. Leventakou, et al. Association of early life exposure to phthalates with obesity and cardiometabolic traits in childhood: sex specific associations. *Frontiers in public health*, 6:327, 2018.

- M. Vrijheid, S. Fossati, L. Maitre, S. Márquez, T. Roumeliotaki, L. Agier, S. Andrusaityte, S. Cadiou, M. Casas, M. de Castro, et al. Early-life environmental exposures and childhood obesity: an exposome-wide approach. *Environmental Health Perspectives*, 128(6):067009, 2020.
- B. Wu, Y. Jiang, X. Jin, and L. He. Using three statistical methods to analyze the association between exposure to 9 compounds and obesity in children and adolescents: Nhanes 2005-2010. *Environmental Health*, 19(1):1–13, 2020.
- T. C. Yang, K. E. Peterson, J. D. Meeker, B. N. Sánchez, Z. Zhang, A. Cantoral, M. Solano, and M. M. Tellez-Rojo. Exposure to bisphenol a and phthalates metabolites in the third trimester of pregnancy and bmi trajectories. *Pediatric obesity*, 13(9):550–557, 2018.
- E. B. Ye’elah, D. A. Doherty, K. M. Main, H. Frederiksen, J. A. Keelan, J. P. Newnham, and R. J. Hart. The influence of prenatal exposure to phthalates on subsequent male growth and body composition in adolescence. *Environmental research*, 195:110313, 2021.
- Y. Zhang and Q. Yang. An overview of multi-task learning. *National Science Review*, 5(1):30–43, 2018.